

---

**TURBULENT FLOW CHARACTERISTICS FOR PITCHED BLADE  
TURBINE\*.\*\***Zdzisław JAWORSKI<sup>a</sup>, Ivan FOŘT<sup>b</sup> and Fryderyk STREK<sup>a</sup><sup>a</sup> *Department of Chemical Engineering and Physical Chemistry,  
Technical University of Szczecin, 71065 Szczecin, Poland and*<sup>b</sup> *Department of Chemical and Food Process Equipment Design,  
Czech Technical University, 166 07 Prague 6, Czechoslovakia*

Received August 3rd, 1987

---

Measurements of the velocity of a stirred liquid in turbulent flow were performed for the area surrounding a pitched blade turbine. A cylindrical tank equipped with four standard baffles and the stirrer was used in the study. A number of traces of tracer particles were photographed and used to determine instantaneous values of the radial and axial components of the liquid local velocity. Those values were employed to estimate local values of the radial and axial components of the mean and fluctuating velocities. Analysis of the radial distribution of the fluctuating velocity components revealed the existence of the local isotropy of those components for the entire investigated area upstream and downstream the stirrer. Moreover, the homogeneity of turbulence in the stream entering the stirrer and in the induced stream can be assumed. The discharge stream showed an approximate homogeneous turbulence of intensity over 2 times higher than that for the other streams.

---

Rotational motion of a stirrer causes pressure differences which in turn forces a stirred liquid to flow. This primary flow induces a secondary one and they both create a circulation of the liquid in a tank. Hydrodynamic characteristics of the liquid stream in the surrounding of the stirrer are thus essential for their distribution in the remaining part of the stirred tank and in consequence for the intensity of heat and mass transfer. The published results of investigations of the turbulent flow in baffled tanks are extensive only for the case of the disc turbine stirrer. Only a few data are available for axial stirrers.

A mathematical description of the distribution of the liquid velocity is relatively simple for the laminar flow in non-baffled tanks. The most complicated modelling arises when the turbulent flow in baffled tanks is handled, for besides the three-dimensional field of the mean velocity a non-homogeneous field of the fluctuating velocity is to be described. The distribution of the mean velocity can be presented with a fair approximation by models found in the literature, e.g. refs<sup>1,2</sup>.

---

\* Part LXIII in the series Studies on Mixing; Part LXXII; Collect. Czech. Chem. Commun. 53, 711 (1988).

\*\* Presented at the CHISA '87 Congress, Prague 1987.

The experimental data on the fluctuating velocity in a tank with the pitched blade turbines have been presented by Fořt<sup>3</sup>. The author has concluded that in the space between the stirrer and the tank bottom the local values of the mean velocity as well as those of the fluctuating velocity have been directly proportional to the stirrer speed. The turbulence intensity averaged along the tank radius has been practically independent of the diameter ratio  $d/D$  and has reached values of 29% to 37%.

The preliminary results of the presented study have been reported elsewhere<sup>4</sup>. The following conclusions have been drawn for the liquid stream in the regions located above and below the stirrer: local values of the mean and fluctuating components of the liquid velocity are directly proportional to the stirrer speed, local values of the axial and radial components of the fluctuating velocity are comparable, the magnitude of the fluctuating velocity is significantly higher in the primary flow than in the induced one or in the region above the stirrer. The aim of the study presented was to derive some quantitative information on the distribution of the fluctuating velocity within the stirrer area for the case of baffled tank.

### EXPERIMENTAL

The investigation was performed in the cylindrical tank with the diameter  $D = 0.29$  m. The tank had the flat bottom and was equipped with four baffles  $b = D/10$  in width. The tank was surrounded by a cubicoid thermostat filled with water. Walls of the tank and the thermostat were made of perspex. The stirred liquid was distilled water at temperatures  $20 \pm 1^\circ\text{C}$ . Its level in the tank was  $H = D$ . The stirrers shown in Fig. 1 were located axially in the tank in the distance  $H/4$  from its bottom. The applied drive allowed to adjust the stirrer speed in the range of 5 to  $32\text{ s}^{-1}$  with the accuracy of 1%. The used direction of the stirrer rotation caused the liquid to be pumped down. Two rotational speeds of the pitched blade turbines were chosen for every stirrer diameter  $d$ :  $n = 5.0$  and  $10.0\text{ s}^{-1}$  for  $d/D = 1/3$ ,  $n = 10.0$  and  $16.7\text{ s}^{-1}$  for  $d/D = 1/4$ ,  $n = 15.0$  and  $25.0\text{ s}^{-1}$  for  $d/D = 1/5$ .

The local values of the velocity of the stirred liquid were evaluated by taking photographs of the traces of the aluminium powder of grain size amounting to  $10^{-4}$  m which was suspended in water. The illumination of the space around the stirrer was obtained by means of two lamps and two vertical diaphragms shown in Fig. 2. The axis of the camera was located horizontally and perpendicularly to the illuminated strip. Owing to the application of the narrow illuminating beam the pictures obtained corresponded to the projection of the traces on the vertical plane of the tank intersection. The exposure time  $\tau$  was  $1/60$  s with variations of  $\pm 2\%$ .

The investigation was limited to the rectangular area which had a height of about  $H/5$ . It was horizontally extended from the tank axis to about a half of the tank radius. From this area three regions were selected. The first one was spread out over the horizontal symmetry axis of the stirrer, the remaining two were placed below this elevation, see Fig. 3.

### THEORETICAL

The basic assumption made in the study was the rotational symmetry of the field of the liquid velocities in the surrounding area of the stirrer. The local and instantana-

neous values of the radial  $v_r$  and axial  $v_z$  components of the liquid velocity were derived from the measurements of the horizontal length  $x_i$  and vertical one  $y_i$  of

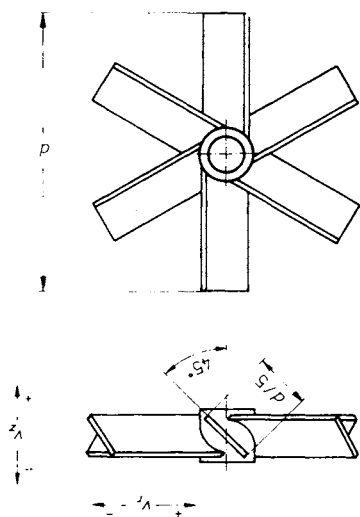


FIG. 1  
Pitched blade turbine stirrer

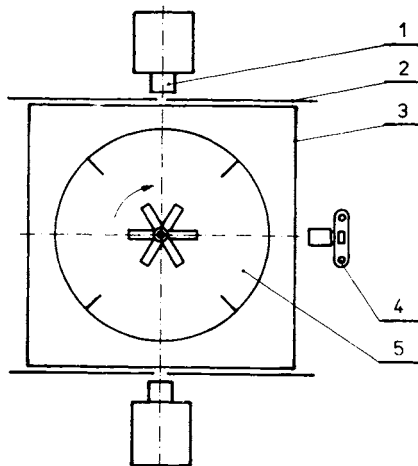


FIG. 2  
Sketch of experimental equipment; 1 lamp, 2 diaphragm, 3 thermostat, 4 camera, 5 stirred tank

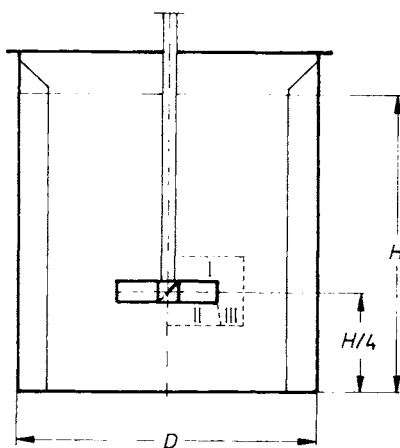


FIG. 3  
Stirred tank and investigated regions

the individual trace in the pictures:

$$v_{ri} = x_i/\tau, \quad (1)$$

$$v_{zi} = y_i/\tau. \quad (2)$$

The calculated values of  $v_r$  and  $v_z$  were assigned to  $r_i$ ,  $z_i$  coordinates of the centre of the individual trace. The sign of the  $v_r$ ,  $v_z$  components was assumed according to Fig. 1 in order to handle mainly the positive value of the velocities.

The above mentioned equations are valid under the assumption that the trajectory of liquid particles is identical with the one of the tracer particles. A deflection of both trajectories could be mainly caused by the gravitational force and by the centrifugal force in the turbulent vortex motion. The settling velocity of the applied powder particles in water is lower than 0.01 m/s, i.e. about 2% of the mean value of the axial velocity. The authors<sup>5</sup> concluded from their experiments conducted in the similar conditions to those described above that the slip velocity of marble particles of the diameter  $11 \cdot 10^{-4}$  m was about 2% of the liquid velocity. Thus for the 10-fold smaller particles applied in the described investigations that deflection could be expected smaller than 2% because of their lower settling velocity. In the opinion of the authors<sup>6</sup> the motion of solid particles in the vicinity of axial turbines is very complex and the path deflections for the particles of liquid and tracer cannot be exactly predicted. On the basis of the above considerations, the average error of the evaluation of the instantaneous values for  $v_r$  and  $v_z$  was estimated about 5%.

About 20 pictures made for constant stirrer speed were analysed separately for the regions above and under the stirrer in order to obtain the representative values of the mean velocity and the fluctuating one. The investigated area was divided by means of vertical lines into subregions. The width of every subregion was chosen initially 0.002 m and subsequently 0.004 m. It was assumed that the width and height of the subregion were small enough to enable the evaluation of the local components  $\langle v_r \rangle$  and  $\langle v_z \rangle$  of the mean from the instantaneous values:

$$\langle v_r \rangle = \frac{1}{N} \sum_{i=1}^N v_{ri}, \quad (3)$$

$$\langle v_z \rangle = \frac{1}{N} \sum_{i=1}^N v_{zi}. \quad (4)$$

The number  $N$  of experimental data (traces) varied from 14 to 46 for the individual subregion of the width 0.004 m. The data were obtained from the subsequent pictures made for the constant speed and size of the stirrers. The arithmetic means  $\langle r \rangle$ ,  $\langle z \rangle$  derived from the  $N$  values of the  $r_i$  and  $z_i$  coordinates were accepted as the coordinates of  $\langle v_r \rangle$  and  $\langle v_z \rangle$ . Such a method of deriving the local values for the mean

velocity components can introduce some additional errors when there is a markedly non-linear radial profile of this velocity. This was the case only for a small part of the discharge stream in the region II. The average error of the evaluation of  $\langle v_r \rangle$  and  $\langle v_z \rangle$  values was estimated to be about 8%.

The statistical definition of the variance was adopted in the evaluation of the radial and axial components of the fluctuating velocity in the subsequent subregions:

$$v'_r \cong \sqrt{\langle v_r'^2 \rangle} = \left( \frac{1}{N-1} \sum_{i=1}^N (v_{ri} - \langle v_r \rangle)^2 \right)^{1/2}, \quad (5)$$

$$v'_z \cong \sqrt{\langle v_z'^2 \rangle} = \left( \frac{1}{N-1} \sum_{i=1}^N (v_{zi} - \langle v_z \rangle)^2 \right)^{1/2}, \quad (6)$$

One can suppose that owing to the adoption of the  $\langle v_r \rangle$  and  $\langle v_z \rangle$  values as the representatives for the whole subregion the estimates  $\langle v'^2 \rangle$  of the fluctuating velocity components would be higher than the real ones. These differences could become distinct in the case of  $\langle v_z'^2 \rangle$  because of the steep gradient of the  $z$ -component of the mean velocity in the region II. The magnitude of the relative error of the evaluation of fluctuating velocity is also influenced by its 2- to 4-times lower value as compared with the mean velocity. It was adopted that the evaluated components of the fluctuating velocity are rather too high and that the relative error of their estimation is about 25%.

## RESULTS AND DISCUSSION

In the first stage of the elaboration of the pictures the width  $\Delta r$  of the subregions was established. Its value initially adopted was 0.002 m. However, the number of traces  $N$  in some subregions fell then below 6 and this could cause significant errors in evaluation of local values of the calculated velocity components  $\langle v_r \rangle$ ,  $\langle v_z \rangle$ ,  $v'_r$ ,  $v'_z$ . The same calculation was carried out for the width  $\Delta r = 0.004$  m and the comparison of results obtained for both widths was done. An example of such comparison for the axial components of the mean and fluctuating velocities in the regions II and III is shown in Figs 4, 5.

The similar consistency of the calculation results for both widths was obtained for the other speed and size of stirrer. However, the dispersion of the fluctuation velocity values was somewhat higher in the case of the smaller width when the number  $N$  was below 10. In the further calculations the width  $\Delta r = 0.004$  m was adopted.

The radial and axial components of the mean velocity were then calculated in order to compare them with the literature data. Following the paper<sup>3</sup> the components were presented in the dimensionless form  $V_r$ ,  $V_z$  by relating them to the speed of the stirrer

tip:

$$V_r = \langle v_r \rangle / \pi n d, \quad (7)$$

$$V_z = \langle v_z \rangle / \pi n d. \quad (8)$$

Some examples of the radial profile of these components for the stirrer diameter  $d = D/4$  are shown in Figs 6, 7. For this stirrer the highest differences in the distribu-

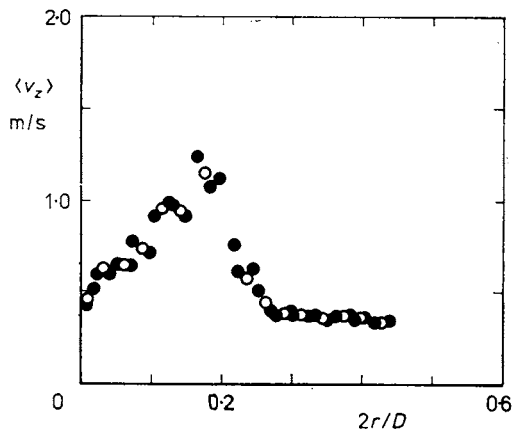


FIG. 4

Example of  $\langle v_z \rangle$  distribution obtained for  $n = 10.0 \text{ s}^{-1}$  and two subregion widths,  $d/D = 1/4$ , regions II, III.  $\Delta r$ , m:  $\circ$  0.004;  $\bullet$  0.002

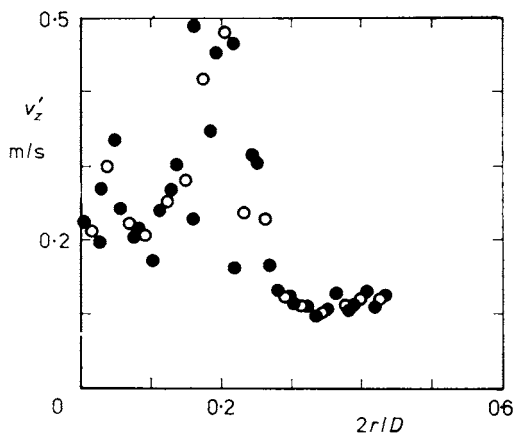


FIG. 5

Example of  $v'_z$  distribution obtained for  $n = 10.0 \text{ s}^{-1}$  and two subregion widths,  $d/D = 1/4$ , regions II, III.  $\Delta r$ , m:  $\circ$  0.004;  $\bullet$  0.002

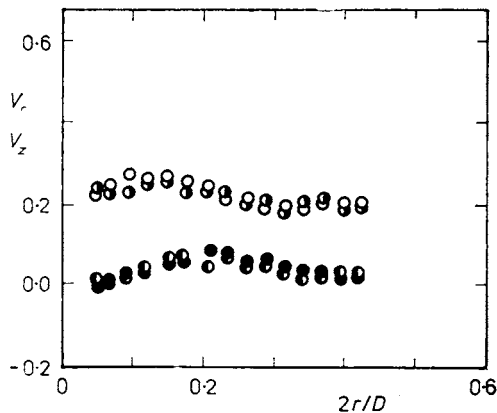


FIG. 6

Radial profile of dimensionless mean velocity components above the stirrer,  $d/D = 1/4$ , region I.  $n$ ,  $\text{s}^{-1}$ : for  $V_r$ :  $\bullet$  10.0;  $\circ$  16.7, for  $V_z$ :  $\circ$  10.0;  $\bullet$  16.7

tion of the components for the applied stirrer speeds were noticed. They became most marked in a part of the discharge stream. For the other stirrers the dimensionless components obtained for different stirrer speed did not differ more than 10% from the average value of the mean velocity. The shape of the velocity profiles was consistent with the experimental data<sup>7</sup>. In order to compare them quantitatively the pumping capacity  $\dot{V}_p$  and primary flow rate number  $Kp$  were computed numerically by means of the relations

$$\dot{V}_p = \int_0^{r_1} 2\pi r \langle v_z \rangle dr, \quad (9)$$

$$Kp = \dot{V}_p / nd^3. \quad (10)$$

The  $Kp$  values for every speed and size of stirrer were computed separately for the region I upstream the stirrer and for the region II of the discharge stream. The  $r_1$  value for the upper limit of the integral was derived by projection of the outer edge of the stirrer blade on the line connecting two neighbouring points with the mean coordinates  $\langle r \rangle$ ,  $\langle z \rangle$ . The projection direction agreed with the linearly interpolated direction of the mean velocity vector. The computed values are presented graphically in Fig. 8 together with the literature correlation<sup>8</sup>. It can be noticed that in the relation to the correlation data the computed  $Kp$  values for the discharge stream are higher up to 10% and for the region I they are lower up to 20%. The dif-

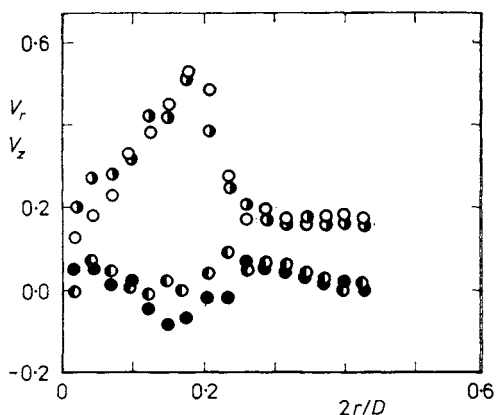


FIG. 7

Radial profile of dimensionless mean velocity components below the stirrer,  $d/D = 1/4$ , regions II, III.  $n$ ,  $s^{-1}$ : for  $V_r$ : ● 10.0; ○ 16.7, for  $V_z$ : ○ 10.0; ● 16.7

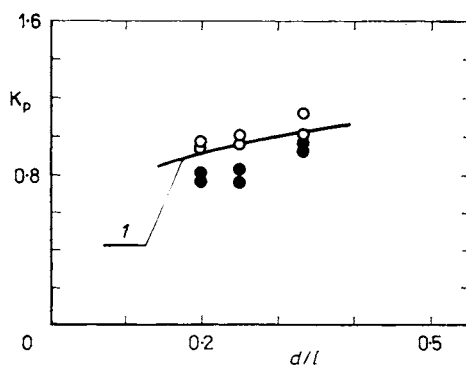


FIG. 8

Primary flow rate number  $Kp$  vs  $d/D$  ● region I (above the stirrer), ○ region II (below the stirrer), 1 literature<sup>8</sup> correlation

ferences were brought about mainly by the simplified method of deriving the  $r_1$  value, for in that method the curvature of stream lines was neglected. This led to the noticeable underrating of the  $r_1$  and also  $K_p$  values for the region I as well as to

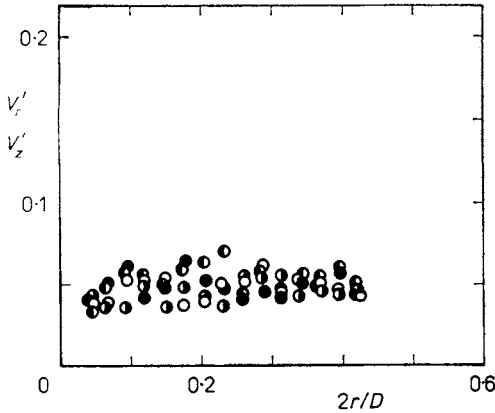


FIG. 9

Radial profile of dimensionless fluctuating velocity components for the area above the stirrer,  $d/D = 1/4$ , region I,  $n, s^{-1}$ : for  $V_r'$ : ● 10.0; ● 16.7, for  $V_z'$ : ○ 10.0, ● 16.7

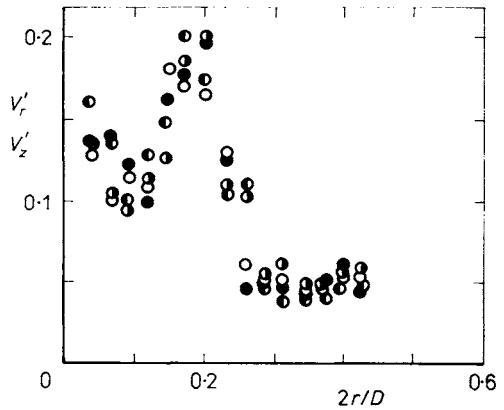


FIG. 10

Radial profile of dimensionless fluctuating velocity components for the area below the stirrer,  $d/D = 1/4$ , regions II, III,  $n, s^{-1}$ : for  $V_r'$ : ● 10.0; ● 16.7, for  $V_z'$ : ○ 10.0, ● 16.7

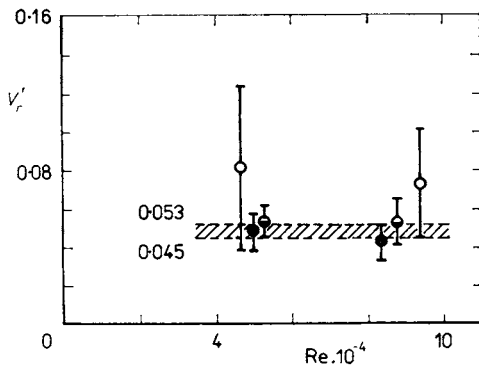


FIG. 11

Comparison of the  $V_r'$  values obtained for the region I. ○ mean value, |—| confidence interval, ○  $d/D = 1/3$ , ●  $d/D = 1/4$ , ●  $d/D = 1/5$

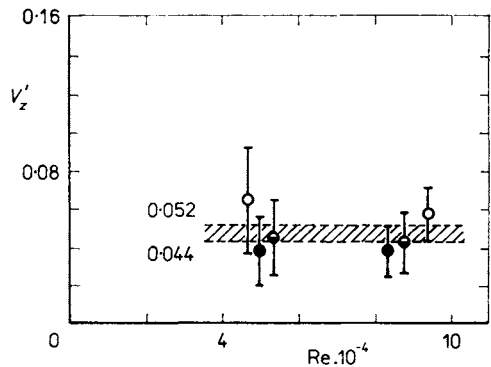


FIG. 12

Comparison of the  $V_z'$  values obtained for the region I. ○ mean value, |—| confidence interval, ○  $d/D = 1/3$ , ●  $d/D = 1/4$ , ●  $d/D = 1/5$



the overestimation of  $r_1$  and  $K_p$  in the case of the discharge stream. That comparison can be recognized as a proof of correctness of the measurement method applied in the study.

The final purpose of the data processing was gaining some information on the distribution of the fluctuating velocity within the investigated regions. In the literature two basic relation velocities can be found; the stirrer tip speed<sup>9</sup> and the local mean velocity<sup>3</sup>. The distribution of the  $\langle v_r \rangle$ ,  $\langle v_z \rangle$  and  $v'_r$ ,  $v'_z$  velocities in the discharge stream justified rather the choice of the stirrer tip velocity. Although the radial profiles of the fluctuating velocity components and the mean velocity were similar, the profile of their ratio had evident minimum for that  $r$  where the mean velocity reached its maximum. In the regions I and III both relation velocities led to similar results. Thus the fluctuating velocity components were related to the stirrer tip velocity:

$$V'_r = \langle v_r'^2 \rangle^{1/2} / \pi n d, \quad (11)$$

$$V'_z = \langle v_z'^2 \rangle^{1/2} / \pi n d. \quad (12)$$

An example of the distribution of the dimensionless components  $V'_r$  and  $V'_z$  is shown in Figs 9, 10 for the stirrer diameter  $d = D/4$ . Similar distributions were obtained for the other stirrer diameters.

The analysis of those distributions revealed that in the region I above the stirrer, e.g. Fig. 9, the values on both dimensionless components  $V'_r$  and  $V'_z$  were grouped around the value of 0.05 independently of the subregion and the stirrer speed. That hypothesis was verified by means of the statistical t-test at the 0.95 confidence level. The mean values for  $V'_r$  and  $V'_z$  for all 15 subregions were calculated for constant values of  $d/D$  and  $n$ . For all variants of the speed and size of stirrer the differences of the local values from their mean were contained within their confidence interval both for  $V'_r$  and  $V'_z$ . The results for the region I were collected in Figs 11 and 12.

It could be presumed that the larger is the stirrer the higher are the dimensionless components  $V'_r$  and  $V'_z$ . However, their increments appeared non-significant statistically because a common part of all confidence intervals existed irrespective of  $d/D$  and  $n$ . That common part was shaded and its limits were given for  $V'_r$  and  $V'_z$  in Figs 11 and 12. A close agreement between the common intervals for both components can be noticed. The appropriate statistical tests made separately for each variant with constant  $d/D$  and  $n$  value resulted in the non-significant differences between  $V'_r$  and  $V'_z$ . Those conclusions suggest that the local isotropy of both components of the fluctuating velocity appears in the region I above the stirrer and is accompanied by the homogeneous turbulence. Since the procedure of the determination of fluctuating velocity components rather overestimates their values the lower limit of the common ranges was adopted as a representative value

$$(V'_r)_I = (V'_z)_I = 0.045. \quad (13)$$

The distribution of the dimensionless components  $V'_r$  and  $V'_z$  for the regions II and III below the stirrer was for all the studied variants similar to that shown in Fig. 10. Those components in the individual subregions took similar values also in the region III. The statistical procedure similar to that described above was employed

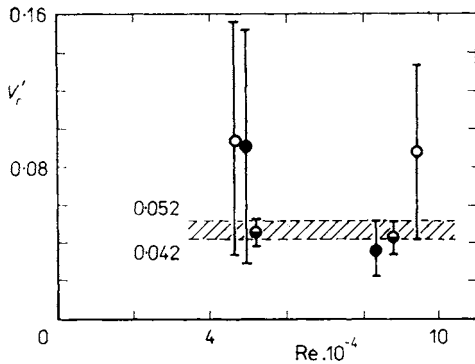


FIG. 13

Comparison of the  $V'_r$  values obtained for the region III.  $\circ$  mean value,  $|—|$  confidence interval,  $\circ$   $d/D = 1/3$ ,  $\bullet$   $d/D = 1/4$ ,  $\bullet$   $d/D = 1/5$

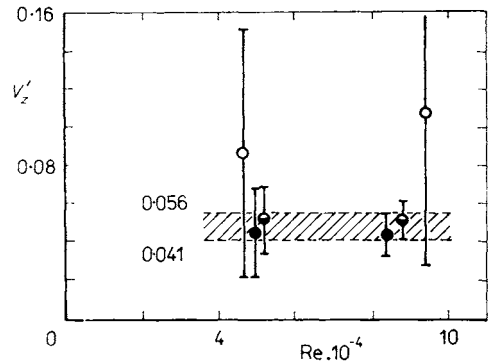


FIG. 14

Comparison of the  $V'_z$  values obtained for the region III.  $\circ$  mean value,  $|—|$  confidence interval,  $\circ$   $d/D = 1/3$ ,  $\bullet$   $d/D = 1/4$ ,  $\bullet$   $d/D = 1/5$

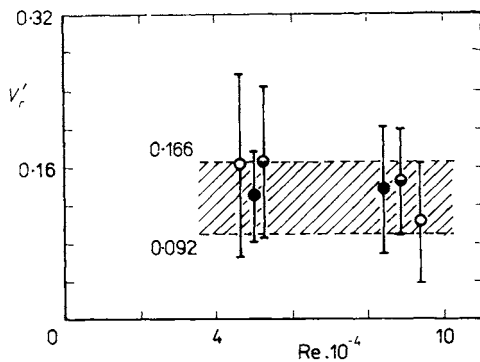


FIG. 15

Comparison of the  $V'_r$  values obtained for the region II.  $\circ$  mean value,  $|—|$  confidence interval,  $\circ$   $d/D = 1/3$ ,  $\bullet$   $d/D = 1/4$ ,  $\bullet$   $d/D = 1/5$

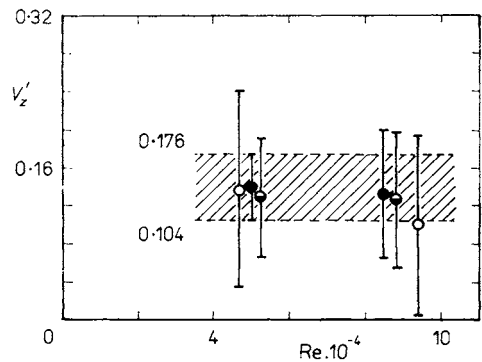


FIG. 16

Comparison of the  $V'_z$  values obtained for the region II.  $\circ$  mean value,  $|—|$  confidence interval,  $\circ$   $d/D = 1/3$ ,  $\bullet$   $d/D = 1/4$ ,  $\bullet$   $d/D = 1/5$

to the data for the induced stream. The same results concerning the local isotropy and homogeneous turbulence were obtained. Some of them are presented in Figs 13 and 14. The common part of the confidence intervals also contained the value

$$(V_r')_{III} = (V_z')_{III} = 0.045. \quad (14)$$

The dimensionless components  $V_r'$  and  $V_z'$  reached in the region II markedly higher values and broader dispersion than in the other regions. Those observations confirm the role of stirrer as a turbulence generator. The majority of the  $V_r'$  and  $V_z'$  values for the individual subregion was distributed in the range from 0.10 to 0.15. Maximum values of  $V_r'$  and  $V_z'$  were close to 0.20 and occurred for that radial coordinate  $r_{\max}$  where the mean axial velocity reached its maximum. The statistical tests did not reject the local isotropy of the fluctuating velocity components or the homogeneity of turbulence in any of the studied subregion. The mean values of the components and the respective confidence levels are presented in Figs 15, 16. The shaded common ranges are similar for  $V_r'$  and  $V_z'$  but their values are over 2 times higher than in the regions I and III. The representative value of those components was adopted close to the lower limits of the common ranges, according to the remarks given earlier about the errors of the evaluation of the fluctuating velocity components. The relation (15) was proposed with the restriction that for the radial coordinate  $r_{\max}$  the components can even reach the value of about 0.20:

$$(V_r')_{II} = (V_z')_{II} = 0.11. \quad (15)$$

From the analysis of the confidence intervals shown in Figs 11 to 16 one can say that the broadest dispersion of the values for  $V_r'$  and  $V_z'$  were usually found for the stirrer diameter  $d = D/3$ . This could be partially caused by the low relation velocity  $\pi nd$  which resulted from the requirement of the similar range of the Reynolds number for all the stirrers. The second reason could be the larger size of the trailing vortex produced by that stirrer.

The values of turbulence intensity  $v_z'/\langle v_z \rangle$  averaged for the region II and III were close to those obtained earlier<sup>3</sup>. The authors<sup>10</sup> using hot-film anemometry have given the values of the dimensionless fluctuating velocity for the disc turbine ranging from 0.10 to 0.18 in the discharge stream and from 0.036 to 0.053 in the remaining tank space. Applying the same technique the authors<sup>11</sup> have proved that the ranges from 0.10 to 0.34 for the discharge stream and from 0.05 to 0.08 in the rest of the tank are valid. It can be assumed that the values of the dimensionless fluctuating velocity for the pitched blade turbine stirrer are lower than for the disc turbine one. However, the ratio of those velocities in the examined streams is similar for both stirrers.

## CONCLUSIONS

- 1) The presented experimental data support the assumption of the local isotropy of the fluctuating velocity components  $V'_r$  and  $V'_z$  for the studied regions surrounding the pitched blade turbine stirrers.
- 2) In the region I above the stirrer and in the induced stream III homogeneous turbulence was confirmed; its scale is described by relations (13) and (14).
- 3) The discharge stream showed approximate homogeneity and more intensive turbulence, its scale is given in the relation (15).

## LIST OF SYMBOLS

$b$	baffle width, m
$d$	stirrer diameter, m
$D$	tank diameter, m
$H$	liquid depth in tank, m
$K_p$	primary flow rate number
$n$	rotational speed of stirrer, $s^{-1}$
$N$	number of experimental data for subregion
$r$	radial coordinate, m
$v$	velocity of stirred liquid, $m\ s^{-1}$
$v'$	fluctuating velocity of stirred liquid, $m\ s^{-1}$
$V$	dimensionless mean velocity
$V'$	dimensionless fluctuating velocity
$\dot{V}_p$	pumping capacity of stirrer, $m^3\ s^{-1}$
$x$	horizontal length of tracer path, m
$y$	vertical length of tracer path, m
$z$	axial coordinate, m
$\nu$	kinematic viscosity of stirred liquid, $kg\ m^{-1}\ s^{-1}$
$\tau$	exposure time of photographs, s
$Re_m = nd^2/\nu$	Reynolds number for mixing
$\langle \rangle$	mean value for subregion

## Subscripts

$i$	summation index
$r$	radial component of liquid velocity
$z$	axial component of liquid velocity
$l$	upper limit of integration
I	region above the stirrer
II	region of the discharge stream
III	region of the induced stream

## REFERENCES

1. Platzer B., Noll G.: *Maschinenbautechnik* 32, 206 (1983).
2. Jaworski T.: *Zesz. Nauk. WSI Opole, Mechanika* 33, 79 (1987).

3. Fořt I.: Collect. Czech. Chem. Commun. 36, 2914 (1971).
4. Jaworski Z., Fořt I., Stręk F.: *Proc. XII Polish Conference on Chemical Engineering, Poznan, 1986*; p. 169.
5. Schwartzberg H. G., Treybal R. E.: Ind. Eng. Chem. Fund. 7, 1 (1968).
6. Chang T. P. K., Watson A. T., Tatterson G. B.: Chem. Eng. Sci. 40, 277 (1985).
7. Fořt I. in: *Mixing: Theory and Practice* (V. W. Uhl and J. B. Gray, Eds), Vol. III, Chapter 14. Academic Press, New York 1986.
8. Medek J., Fořt I.: Collect. Czech. Chem. Commun. 44, 3077 (1979).
9. Liepe F.: *Advances in Mechanics*, Vol. 4, No. 4. Wydawnictwo Naukowe, Warsaw 1981.
10. Liepe F., Möckel H. O., Winkler H.: Chem. Techn. (Leipzig) 23, 231 (1971).
11. Barthole J. P., Maisonneuve J., Gence J. N., David R., Mathieu J., Villermaux J.: Chem. Eng. Fund. 1, 17 (1982).